Close coupling calculations on rotational excitation and inversion of NH_3 by collisions with Ar

G. C. M. van der Sanden, P. E. S. Wormer, and A. van der Avoird
Institute of Theoretical Chemistry, University of Nijmegen, Toernooiveld, 6525 ED Nijmegen, The Netherlands

J. Schleipen and J. J. ter Meulen
Department of Molecular and Laser Physics, University of Nijmegen, Toernooiveld, 6525 ED Nijmegen, The Netherlands

(Received 6 July 1992; accepted 31 July 1992)

State-to-state total cross sections for rotational excitation and inversion of NH_3 by collisions with Ar have been calculated within the accurate close coupling framework. The inversion motion in NH_3 was included both via a delta function model and by taking the inversion coordinate explicitly into account. We used an *ab initio* potential and a potential in which one term in the angular expansion of the *ab initio* potential is scaled in order to reproduce spectroscopic data. At the energies of these calculations the delta function model is found to be in nearly quantitative agreement with the "exact" inversion results. Comparison with experiment shows the original *ab initio* potential to be better than the scaled one. The state-to-state cross sections for ortho-NH_3 are in general accord with the measurements. For para-NH_3 the agreement is good also, but the relative magnitudes of the cross sections for transitions to the $\pm$ inversion states of the same rotational level are not reproduced correctly for all levels.

I. INTRODUCTION

The last few years it has become possible to obtain state-to-state cross sections for transitions between rotation–inversion ($j_k^{\pm}$) states of NH_3, induced by collisions with various perturbers. Advances in molecular beam techniques and in laser spectroscopy have made it feasible to discriminate between the symmetric (+) and antisymmetric (−) states of the inversion doublets. The close coupling (CC) method for the accurate quantum mechanical treatment of the problem has been well established theoretically for quite some time. However, computer systems that meet the computational demands have only recently become available.

In this paper we consider collisions of NH_3 with Ar. This study was undertaken mainly for two reasons. First, comparison of theoretical results with experimental data enables us to determine the accuracy of an *ab initio* intermolecular potential energy surface,[1] in the region that is probed in scattering experiments. In addition, we used a slightly different potential in order to gain some understanding of the sensitivity of the cross sections to variations in the potential surface. This second potential contains a scaling parameter that was chosen to account for spectroscopic data regarding the bound states of Ar–NH_3. In particular, we wanted to see whether a variation that improved bound state results would also improve the outcome of the scattering calculations.

Second, we investigate how the description of the umbrella inversion of NH_3 influences the cross sections. Until now, this inversion has been included in scattering calculations on NH_3 only via a model in which the inversion-tunneling wave function is a linear combination of two delta functions centered at the equilibrium positions (Davis and Boggs,[2] Green[3]). Although the model has its justification in the fact that the period for inversion is much longer than the duration of a collision, it was not clear whether experimentally found deviations from predicted propensity rules could not be attributed to the neglect of the inversion motion in the description of the intermolecular potential.[4,5] Here we take the inversion degree of freedom explicitly into account, in order to assess how severe an approximation is made in neglecting it.

Finally, we have performed some calculations using the much cheaper coupled states (CS) approximation, to find out how this approximation affects the calculated cross sections. In calculations on He–NH_3 using the CS method[6] certain theoretical cross sections are found to vanish or almost vanish, whereas the experimental cross sections are significantly different from zero.[4] By applying the CS approximation, together with the full CC method on the same Ar–NH_3 potential surface, we can establish to what extent deviations are caused by the theoretical scattering method.

II. THEORY

The coordinate system used in the CC method is the space-fixed frame.[7] The vector **R**, with polar angles (β,α) in this frame, points from the NH_3 center of mass to the Ar nucleus. The orientation of NH_3 is given by the Euler angles $(\gamma,\vartheta,\varphi)$, where γ and ϑ are the usual spherical polar angles of the symmetry axis of NH_3 with respect to the space fixed frame and φ is the third Euler angle describing a rotation of the symmetric top around its symmetry axis. In the geometry $\gamma=\vartheta=\varphi=0$, the nitrogen is on the posi-

 0021-9606/92/216460-09$006.00

tive z-axis and one of the protons is in the xz plane with a positive x-component. The inversion coordinate ρ is defined as the angle between the C_3 axis and one of the N–H bonds.

The rotation–inversion scattering Hamiltonian can be written as

$$\hat{H}=\hat{H}_{\text{umb}}(\rho)+\hat{H}_{\text{vdw}}(\gamma,\vartheta,\varphi,R,\beta,\alpha,\rho). \tag{1}$$

The Hamiltonian for the umbrella motion of the NH_3 monomer, which depends only on the internal coordinate ρ, is designated by $\hat{H}_{\text{umb}}$. It describes both the fast umbrella vibration (ν_2) and the slow inversion tunneling. If the threefold symmetry is retained and the N–H distance is kept fixed at r_0, $\hat{H}_{\text{umb}}$ is given by[8,9]

$$\hat{H}_{\text{umb}}=-\tfrac{1}{2}\hbar^2 g(\rho)^{-1/2}\frac{\partial}{\partial\rho}I_{\rho\rho}^{-1}(\rho)g(\rho)^{1/2}\frac{\partial}{\partial\rho}+V_{\text{umb}}(\rho), \tag{2}$$

where

$$g(\rho)=I_{xx}(\rho)I_{yy}(\rho)I_{zz}(\rho)I_{\rho\rho}(\rho), \tag{3a}$$

$$I_{xx}(\rho)=I_{yy}(\rho)=3m_H r_0^2(\tfrac{1}{2}\sin^2\rho+\zeta\cos^2\rho), \tag{3b}$$

$$I_{zz}(\rho)=3m_H r_0^2\sin^2\rho, \tag{3c}$$

$$I_{\rho\rho}(\rho)=3m_H r_0^2(\cos^2\rho+\zeta\sin^2\rho), \tag{3d}$$

$$\zeta=m_N/(3m_H+m_N). \tag{3e}$$

Here $g(\rho)$ is the determinant of the metric tensor g $=\text{diag}(I_{xx},I_{yy},I_{zz},I_{\rho\rho})$ in a curvilinear coordinate system; m_H and m_N are the masses of the hydrogen and nitrogen nuclei. The quantities I_{xx}, I_{yy}, and I_{zz} are the moments of inertia of NH_3, which depend on the inversion coordinate ρ. The generalized moment of inertia $I_{\rho\rho}$ is associated with the umbrella motion and depends also on the inversion coordinate. The double well potential $V_{\text{umb}}(\rho)$ is represented by a harmonic force field augmented by a Gaussian

$$V_{\text{umb}}(\rho)=\tfrac{1}{2}k(\rho-\tfrac{1}{2}\pi)^2+a\exp[-b(\rho-\tfrac{1}{2}\pi)^2]. \tag{4}$$

The parameters k, a, and b are chosen such that the measured inversion tunneling splitting in the ν_2 ground state and both transitions to the ν_2 first excited state are reproduced to an accuracy better than 0.1%. The form of the resulting potential is shown in Fig. 1.

The associated eigenvalue problem is solved in Ref. 10 with the use of a basis of functions $\sin m\rho$ ($m=1,\ldots,100$). Here we consider only the lowest two eigenfunctions $|\nu\rangle$, also shown in Fig. 1. They describe the lower and upper inversion states that are separated by 0.8 cm^{-1}. The lowest of the two, which is designated by $\nu=+$, is symmetric with respect to $\rho\rightarrow\pi-\rho$. The upper level, designated by $\nu=-$, is antisymmetric with respect to this operation.

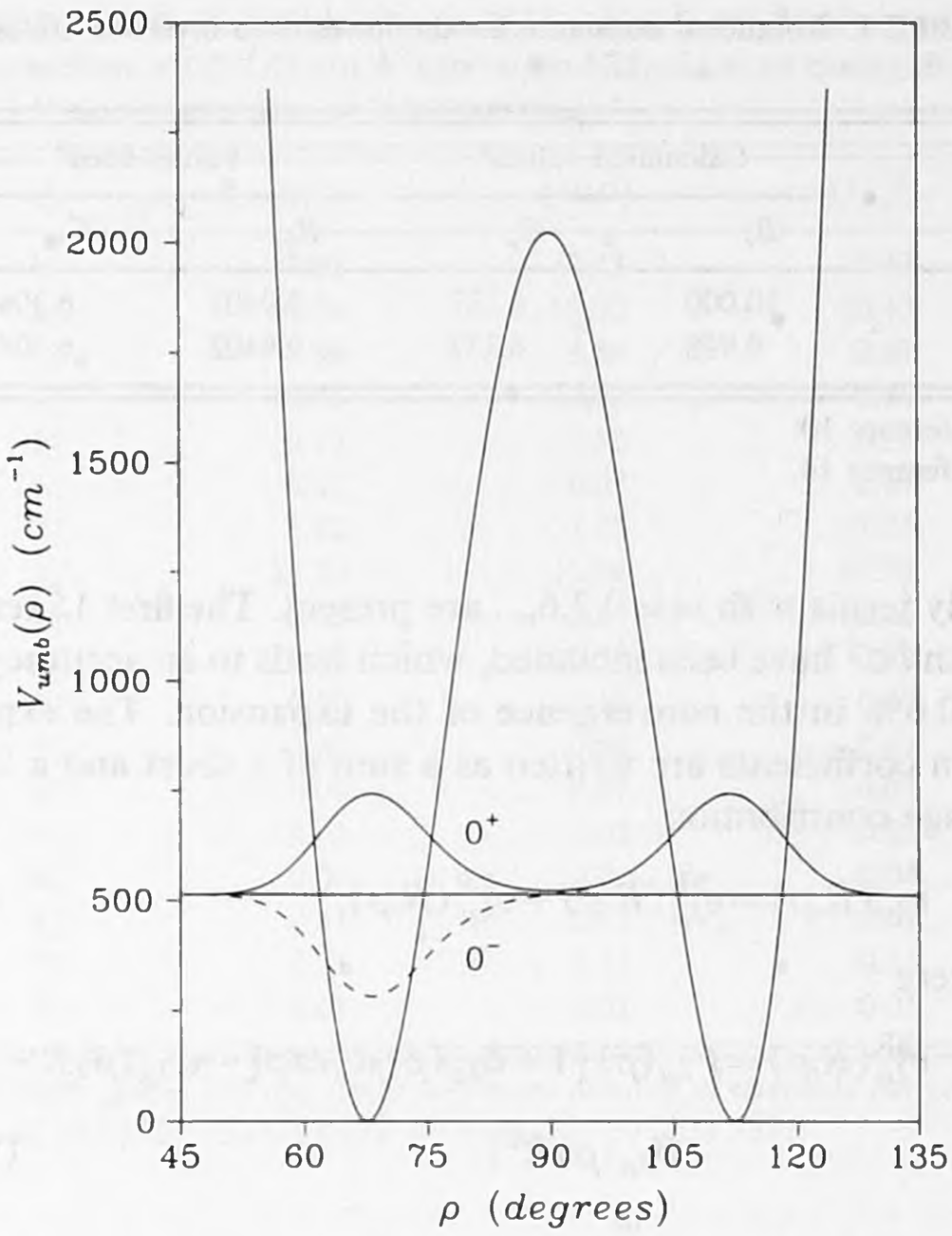

FIG. 1. Double well potential $V_{\text{umb}}(\rho)$ for the NH_3 umbrella motion [cf. Eq. (4)] and the two lowest eigenfunctions of $\hat{H}_{\text{umb}}(\rho)$ [cf. Eq. (2)]. Wave functions in arbitrary units and zero coinciding with the corresponding energy.

The van der Waals Hamiltonian can be written as

$$\hat{H}_{\text{vdw}}(\gamma,\vartheta,\varphi,R,\beta,\alpha,\rho)=B(\rho)\hat{j}^2+[C(\rho)-B(\rho)]\hat{j}_z^2-\frac{\hbar^2}{2\mu R}\frac{\partial^2}{\partial R^2}R+\frac{\hat{l}^2}{2\mu R^2}+V_{\text{int}}(\gamma,\vartheta,\varphi,R,\beta,\alpha,\rho). \tag{5}$$

The first two terms in $\hat{H}_{\text{vdw}}$ represent the symmetric top Hamiltonian of NH_3. The rotational constants are related to the moments of inertia given in Eq. (3), $B(\rho)=[2I_{xx}(\rho)]^{-1}$ and $C(\rho)=[2I_{zz}(\rho)]^{-1}$. The third and fourth term give the kinetic energy of the "diatom," with $\hat{l}$ being the relative angular momentum. The intermolecular potential V_{int} is expanded in spherical harmonics $Y_{\lambda\mu}$,

$$V_{\text{int}}(R,\Theta,\Phi,\rho)=\sum_{\lambda\mu}v_{\lambda\mu}(R,\rho)Y_{\lambda\mu}(\Theta,\Phi), \tag{6}$$

where Θ and Φ are the polar angles of the Ar projectile with respect to the principal axes frame of the NH_3 rotor. In the space fixed frame $Y_{\lambda\mu}(\Theta,\Phi)$ becomes

$$Y_{\lambda\mu}(\Theta,\Phi)=\sum_{\nu}D_{\nu\mu}^{(\lambda)}(\gamma,\vartheta,\varphi)Y_{\lambda\nu}(\beta,\alpha), \tag{7}$$

where $D_{\nu\mu}^{(\lambda)}(\gamma,\vartheta,\varphi)$ is the usual Wigner rotation matrix.[11] The expansion coefficients $v_{\lambda\mu}(R,\rho)$ have been taken from Bulski *et al.*,[1] who calculated the *ab initio* potential for four different umbrella angles ρ, and expanded it in tesseral harmonics. Due to the threefold symmetry of the ammonia

TABLE I. Rotational constants for the lowest two inversion states (in cm^{-1}).

	Calculated values[a]		Values used[b]	
ν	B_ν	C_ν	B_ν	C_n
+	10.000	6.337	9.9402	6.3044
−	9.998	6.337	9.9402	6.3044

[a]Reference 10.
[b]Reference 14.

only terms with $m=0,3,6,...$ are present. The first 15 terms with $l\leqslant 7$ have been included, which leads to an accuracy of $\sim 0.6\%$ in the convergence of the expansion. The expansion coefficients are written as a sum of a short and a long range contribution,

$$v_{\lambda\mu}(R,\rho)=v_{\lambda\mu}^{\mathrm{SR}}(R,\rho)+v_{\lambda\mu}^{\mathrm{LR}}(R,\rho), \tag{8}$$

where

$$v_{\lambda\mu}^{\mathrm{SR}}(R,\rho)=F_{\lambda\mu}(\rho)[1+\delta_{\lambda\mu}(\rho)R]\exp[-\alpha_{\lambda\mu}(\rho)R - \beta_{\lambda\mu}(\rho)R^2], \tag{9a}$$

$$v_{\lambda\mu}^{\mathrm{LR}}(R,\rho)=-\sum_{n=6}^{10} f_n^{\lambda\mu}(R,\rho)C_n^{\lambda\mu}(\rho)R^{-n}. \tag{9b}$$

The $C_n^{\lambda\mu}(\rho)$ are the induction and dispersion coefficients, the $f_n^{\lambda\mu}(R,\rho)$ are Tang and Toennies type damping functions. The values of all coefficients are given in Ref. 1. The rotational constants for a given tunneling state ν are given by

$$B_\nu=\langle\nu|B(\rho)|\nu\rangle$$

and

$$C_\nu=\langle\nu|C(\rho)|\nu\rangle. \tag{10}$$

Their values are listed in Table I.

In the CC method[7] the angular basis functions are usually formed by Clebsch–Gordan coupling of the relative angular momentum functions $Y_{lm_l}(\beta,\alpha)=|lm_l\rangle$ and the symmetric top functions $|jkm\rangle$ to a total angular momentum J with space fixed z-component M. In the case of permutation-inversion symmetry $\mathrm{PI}(D_{3h})$, which we have here, it is convenient to take linear combinations $|jkm\epsilon\rangle$ of the symmetric top functions, defined by

$$|jkm\epsilon\rangle=[2(1+\delta_{k0})]^{-1/2}(|jkm\rangle+\epsilon|j-km\rangle), \tag{11}$$

where $k\geqslant 0$ and $\epsilon=\pm 1$, except for $k=0$ when obviously only $\epsilon=+1$ is allowed.

Since we take the umbrella motion explicitly into account, the basis has to be extended by taking the tensor product with the tunneling functions $\nu(\rho)$,

$$|jklJM\epsilon\nu\rangle=\sum_{m,m_l}|jkm\epsilon\rangle|lm_l\rangle|\nu\rangle\langle jmlm_l|JM\rangle, \tag{12}$$

where $\langle jmlm_l|JM\rangle$ is a Clebsch–Gordan coefficient.[11] From symmetry considerations it follows[3] that the symmetric (antisymmetric) inversion function can combine to a state adapted to $\mathrm{PI}(D_{3h})$ with only one of the two $|jkm\epsilon\rangle$ functions, so that $\epsilon=\mp(-1)^j$ for $\nu=|\pm\rangle$. We can therefore omit the quantum number ν and label the basis functions by $|jklJM\epsilon\rangle$, instead of using the labeling given in Eq. (12). In the CC equations the noninteracting blocks for different J are separated into two parity blocks, each containing channels $(jkl\epsilon)$ having different values of $\epsilon(-1)^{j+k+l}$. States of the free NH_3 can be designated by j_k^ϵ, thereby uniquely specifying the inversion function.

The coupling between the channels that originates from the potential matrix elements is given by

$$V_{j'k'l'\epsilon'}^{jkl\epsilon}=\sum_{\lambda\mu}\langle jklJM\epsilon|v_{\lambda\mu}(R,\rho)Y_{\lambda\mu}(\Theta,\Phi)|j'k'l'JM\epsilon'\rangle. \tag{13}$$

The integration over all the relevant angles $\alpha,\beta,\gamma,\vartheta,\varphi$ is performed, after substitution of Eq. (7), by angular momentum techniques, as is usual in the CC method.[7] In order to calculate the matrix elements between the two tunneling states $\nu(\rho)$ we obtained an analytical representation of the ρ-dependence of the expansion coefficients $v_{\lambda\mu}(R,\rho)$ by fitting, for each value of R, a fifth order polynomial in $\rho-\frac{1}{2}\pi$ through the *ab initio* values of the coefficients for different ρ. The fit contains only even or only odd powers depending on whether $\lambda+\mu$ is even or odd. The matrix elements can then be evaluated as follows:

$$\langle\nu|v_{\lambda\mu}(R,\rho)|\nu'\rangle=\sum_{n=0}^{5}c_n^{\lambda\mu}(R)\langle\nu|(\rho-\tfrac{1}{2}\pi)^n|\nu'\rangle, \tag{14}$$

where the $c_n^{\lambda\mu}(R)$ are the polynomial expansion coefficients. The above relationship between the values of ϵ and ν is used to insert the correct (ν,ν') combination into Eq. (13).

According to Ref. 12 the *ab initio* potential has to be scaled to give good agreement with spectroscopic data for the bound Ar–NH_3 complex. This scaling consists of multiplying the short range parameter F_{33} in Eq. (9a) by a factor of 1.43. Here, calculations have been performed using both the original *ab initio* potential and a modified potential in which the same scaling was applied for all values of the inversion coordinate ρ.

In addition to the calculation with the inversion averaged matrix elements in the way we have just described (henceforth referred to as the "exact" inversion method), we have used the model developed by Davis and Boggs[2] and Green.[3] In this model the inversion functions are taken to be delta functions, $|\pm\rangle=[\delta(\rho-\rho_e)\pm\delta(\rho-\pi+\rho_e)]/\sqrt{2}$, where ρ_e is the value of the inversion coordinate in the equilibrium configuration. In this case the intermolecular potential needs to be known only for the equilibrium angle, since the expansion coefficients, averaged over the inversion functions, are now given by[2,3]

$$\langle\pm|v_{\lambda\mu}(R,\rho)|\pm\rangle=\begin{cases}v_{\lambda\mu}(R,\rho_e), & \text{for } \lambda+\mu \text{ even}\\ 0, & \text{for } \lambda+\mu \text{ odd},\end{cases}$$

$$\langle\pm|v_{\lambda\mu}(R,\rho)|\mp\rangle=\begin{cases}0, & \text{for } \lambda+\mu \text{ even}\\ v_{\lambda\mu}(R,\rho_e), & \text{for } \lambda+\mu \text{ odd}.\end{cases} \tag{15}$$

Using this model for the inversion functions, together with the neglect of the inversion splitting, the scattering equations for para-NH_3 are invariant to a simultaneous change of parity in the incoming and outgoing channels, i.e.,

$$\sigma(j_k^{\epsilon} \rightarrow j_{k'}^{\prime\epsilon'}) = \sigma(j_k^{-\epsilon} \rightarrow j_{k'}^{\prime -\epsilon'}). \tag{16}$$

In the CS method[7] the scattering equations are expressed in a body-fixed coordinate system. The fourth term in the van der Waals Hamiltonian, Eq. (5), is approximated by putting $\hat{l}^2$ $(=\hat{J}^2+\hat{j}^2-2\hat{\mathbf{j}}\cdot\hat{\mathbf{J}})$ equal to $\hat{J}^2$. This implies that the Coriolis interactions are neglected and that Ω, the projection of both $\hat{\mathbf{j}}$ and $\hat{\mathbf{J}}$ on the vector $\mathbf{R}$, is a good quantum number, i.e., there is no coupling between channels with different Ω. The molecular symmetry group of the dimer is thus enlarged from $\mathrm{PI}(D_{3h})$ to the semidirect product of C_∞ with $\mathrm{PI}(D_{3h})$.

III. COMPUTATIONAL ASPECTS

The calculations were carried out with the HIBRIDON inelastic scattering code.[13] The total collision energy E, the maximum value of the total angular momentum J and the values of j and k at which the rotational basis set is truncated, are input parameters of the program. The values for l are then given by triangular inequalities [cf. Eq. (12)]. The program has the possibility of further reducing the size of the basis set as the overall rotation takes up more and more of the available energy. So, from a chosen value of J onwards, the program includes only open channels. To keep the calculations feasible even at higher energies, an interpolation scheme for the total cross sections as a function of J can be used, leading to a substantial reduction of the required cpu time.

The values of the total energies are determined by the two relative kinetic energies attained in the experiment, 280 and 485 cm^{-1}. The ortho-NH_3 with initial state $j=k=0$ has zero internal energy, so the total energies are equal to the relative kinetic energies. The initial $j=k=1$ state of para-NH_3, which is the ground state of this species, has an internal energy of 16.245 cm^{-1}. The total energies are consequently set equal to 296.245 and 501.245 cm^{-1}. The molecular levels in the basis set are retained up to $j=9$ inclusive, with all allowed values of k. This means that for ortho-NH_3 34 levels are included (with a maximum energy of 895 cm^{-1}), 11 of which are asymptotically accessible in the lower, and 19 in the higher energy case. Out of the 66 levels for para-NH_3 (with a maximum energy of 891 cm^{-1}), 24 and 40 levels are accessible, respectively. The J value at which we start to neglect closed channels is 78. The interpolation step size ΔJ is taken to be six, so that calculations are actually performed for $J=0,6,12,\ldots,150$. As explained in Sec. II, the NH_3 inversion is taken into account by calculation of the matrix elements according to the "exact" inversion method, given in Eq. (14), or according to the delta function model, given in Eq. (15).

Convergence with respect to relevant parameters in the propagator, such as the step size ΔR, was better than 1%. Table II shows the dependence of the cross sections on the magnitude of the rotational basis set. Going from a maximum j value of 9 to a maximum value of 11 in the rotational basis set, induced changes in the cross sections of $\sim 6\%$. The neglect of closed channels for $J>78$ did not affect the results. The effect of interpolation step size ΔJ on the cross sections is shown in Table III. The error due to the step size used here is found to be $<5\%$.

TABLE II. Effect of the maximum (j,k) values in the basis set on the cross sections $\sigma(0_0^+ \rightarrow j_k^{\epsilon})$ (in $Å^2$) for ortho-NH_3–Ar at an energy of 485 cm^{-1} ("exact" inversion, *ab initio* potential).[a]

j_k^{ϵ}	(9,9)	(10,9)	(11,9)
1_0^+	7.92	7.43	7.42
2_0^+	10.10	10.50	10.47
3_0^+	3.94	3.84	3.87
4_0^+	0.46	0.52	0.54
5_0^+	0.13	0.13	0.13
6_0^+	0.07	0.07	0.07
3_3^+	1.32	1.25	1.25
3_3^-	11.70	11.96	11.98
4_3^-	2.52	2.27	2.26
4_3^+	0.65	0.72	0.72
5_3^+	0.10	0.10	0.10
5_3^-	0.63	0.60	0.61
6_3^-	0.06	0.07	0.07
6_3^+	0.01	0.02	0.02
6_6^-	0.04	0.04	0.04
6_6^+	0.41	0.42	0.42
7_6^+	0.11	0.13	0.13
7_6^-	0.01	0.01	0.01

[a]RS/6000 model 320 cpu time/maximum number of channels per parity block, (9,9): $24^h/219$, (10,9): $53^h/292$, (11,9): $122^h/372$.

Since the averaging of the rotational constants over the inversion wave functions has a small effect (cf. Table I), we have taken the same value for both inversion states,[14] $B=9.9402$ cm^{-1} and $C=6.3044$ cm^{-1}. The maximum number of channels used in the calculation was 219 per parity block for ortho-NH_3, taking ~ 24 cpu hours for a full calculation, and 441 per parity block for para-NH_3, taking ~ 241 cpu hours on an IBM RS/6000 model 320 workstation.

In the CS calculation we used only the "exact" inversion method. The value of Ω ranged from 0 to 7 for ortho and from 0 to 8 for para; the maximum j value in the rotational basis set was 9 and J was varied from 0 to 150 at an energy of 485 and 501.245 cm^{-1}, respectively. The in-

TABLE III. Effect of the interpolation step size ΔJ on the cross sections $\sigma(0_0^+ \rightarrow j_k^{\epsilon})$ (in $Å^2$) for ortho-NH_3–Ar at an energy of 280 cm^{-1} (delta function model inversion, *ab initio* potential).

j_k^{ϵ}	$\Delta J=1$	$\Delta J=4$	$\Delta J=6$	$\Delta J=8$
1_0^+	10.83	10.93	11.35	9.06
2_0^+	9.02	9.00	8.74	9.63
3_0^+	4.43	4.32	4.34	4.29
4_0^+	0.42	0.40	0.39	0.38
3_3^+	1.64	1.63	1.62	1.59
3_3^-	9.26	9.25	9.33	8.42
4_3^-	3.21	3.33	3.25	3.34
4_3^+	0.25	0.22	0.25	0.24
5_3^+	0.06	0.05	0.05	0.05
5_3^-	0.34	0.36	0.36	0.34

TABLE IV. State-to-state cross sections $\sigma(0_0^+ \rightarrow j_k^\epsilon)$ for ortho-NH_3–Ar in Å^2 at an energy of 280 cm^{-1}. The cross sections given in parentheses are corrected for the incomplete initial state preparation in the measurement, as follows [cf. Eq. (17)]: $\sigma(\rightarrow 1_0^+) = 0.92\sigma(0_0^+ \rightarrow 1_0^+) - 0.08\Sigma_{i\neq 1_0^+}\sigma(1_0^+ \rightarrow i)$, $\sigma(\rightarrow j_k^\epsilon) = 0.92\sigma(0_0^+ \rightarrow j_k^\epsilon) + 0.08\sigma(1_0^+ \rightarrow j_k^\epsilon)$, for $j_k^\epsilon \neq 1_0^+$. A dash (—) in the last column indicates that the corresponding cross section has not been measured.

j_k^ϵ	V_{I}[a]	V_{II}[b]	V_{III}[c]	V_{IV}[d]	Expt.
1_0^+	11.35(7.64)	4.03(1.09)	11.06(7.41)	3.82(0.87)	6.07
2_0^+	8.74(8.69)	13.35(12.65)	8.45(8.42)	13.20(12.49)	6.73
3_0^+	4.34(4.29)	2.56(2.98)	4.16(4.12)	2.51(2.94)	2.19
4_0^+	0.39(0.53)	2.41(2.37)	0.35(0.49)	2.44(2.40)	0.48
3_3^+	1.62(2.24)	0.75(1.53)	1.54(2.17)	0.70(1.53)	3.43
3_3^-	9.33(8.84)	10.10(9.47)	9.04(8.56)	10.65(9.96)	12.23
4_3^-	3.25(3.18)	1.94(1.97)	3.38(3.29)	1.87(1.91)	5.77
4_3^+	0.25(0.33)	0.45(0.51)	0.23(0.32)	0.44(0.50)	1.31
5_3^+	0.05(0.06)	0.39(0.40)	0.06(0.07)	0.41(0.42)	—
5_3^-	0.36(0.36)	0.28(0.28)	0.34(0.35)	0.31(0.31)	—

[a] V_{I}, delta function model inversion, *ab initio* potential.
[b] V_{II}, delta function model inversion, scaled potential.
[c] V_{III}, "exact" inversion *ab initio* potential.
[d] V_{IV}, "exact" inversion, scaled potential.

terpolation step size ΔJ was six as well. The ortho calculation took 45 min on the same workstation, with a maximum of 34 channels per Ω-block, the para calculation took 4 h with a maximum of 66 channels per Ω-block.

IV. RESULTS AND DISCUSSION

The results of the calculations reported here are compared with the results of a crossed molecular beam experiment, which is described in Ref. 15. Differences in population of a specific rotation–inversion state $|i\rangle \equiv j_k^\epsilon$ before and after the collision are measured. The signal is proportional to

$$\Delta n(j) = \sum_{i\neq j} [n(i)\sigma(i\rightarrow j) - n(j)\sigma(j\rightarrow i)], \qquad (17)$$

where $n(j)$ stands for the initial population of state j and $\Delta n(j)$ for the collision induced change in that population. For the experiment to yield pure state-to-state cross sections, only a single state must be initially populated. This requirement, however, cannot be completely met. For ortho-NH_3 the initial state consists of 92% 0_0^+ and 8% 1_0^+ and for para-NH_3 of 95% 1_1^- and 5% 1_1^+. The state-to-state cross sections obtained from the calculations therefore have to be put into Eq. (17), in order to enable comparison with the observed quantities.

Only relative values for the cross sections can be derived from the experiment. To facilitate comparison, the sum of the experimental cross sections is set equal to the sum of the cross sections calculated with the original *ab initio* potential and the "exact" inversion method. The sum contains all cross sections that are actually measured. This sum hardly differs for the scaled and the original *ab initio* potential. The experimental results thus acquired are given in Tables IV, V, and VI and Figs. 2–5, together with the corresponding theoretical values obtained from the CC calculations. The results for ortho-NH_3 are given both for the delta function model and for the "exact" inversion treatment. The experimental error is estimated between 10% and 20%.

Both for ortho and para-NH_3 the scaling in the potential has a large effect. In the case of ortho-NH_3 this effect is about the same for the various cross sections at both energies. Especially transitions to 1_0^+, 2_0^+, 3_0^+, and 4_0^+ are strongly affected in the lower energy case, and transitions to 1_0^+, 3_0^+, and 4_0^+ in the higher energy case. Use of the delta function model for inversion does not affect the influence of the scaling. For para-NH_3 the scaling in the potential decreases some of the cross sections at the lower energy and increases them at the higher energy, for other cross sections it is vice versa. For the lower energy the scaling reduces the size of most of the para cross sections, except for the 2_1^+, 4_4^+, and 4_1^- states. The scaling induces large changes in the relative magnitudes for the ± inversion states for transitions to the 2_1, 3_2, and 4_4 states.

Comparison with the experiment shows that the calculations using the original *ab initio* potential give a better overall agreement than calculations using the scaled potential. Particularly, cross sections to the 1_0^+, 2_0^+, and $2_1^\pm$ states come out better. In a few cases, however, the cross sections from the scaled potential are closer to the experimental ones.

It has been debated whether it is necessary to include higher anisotropic terms, such as a v_{33} term,[16] in the description of the intermolecular potential, since the observed far-infrared Ar–NH_3 spectrum could also be explained with an effective angular potential that contains only terms up to v_{20}.[17] When we look at the results of the scattering calculations, we observe, for example, that in the case of ortho-NH_3 the experimental cross sections $\sigma(0_0^+ \rightarrow 3_3^\pm)$ are reproduced fairly well. In the first Born approximation these transitions are solely due to the v_{33} term in the potential. It seems unlikely that the agreement between experiment and theory could be maintained if this important first order contribution were zero, as it would be when v_{33} would vanish.

Inspection of the influence of the scaling in v_{33} on the cross sections of ortho-NH_3 shows that not only $\Delta j = \Delta k = 3$ transitions are affected, but other transitions as well.

TABLE V. State-to-state cross sections $\sigma(0_0^+ \rightarrow j_k^e)$ for ortho-NH_3–Ar in Å^2 at an energy of 485 cm^{-1}. The corrected cross sections given in parentheses are obtained as indicated in Table IV. A dash (—) in the last column indicates that the corresponding cross section has not been measured.

j_k^e	V_I[a]	V_{II}[b]	V_{III}[c]	V_{IV}[d]	Expt.
1_0^+	7.90(4.30)	5.94(2.40)	7.92(4.33)	5.53(2.04)	4.33
2_0^+	10.20(9.85)	10.73(10.17)	10.10(9.76)	11.02(10.42)	5.72
3_0^+	4.07(4.07)	1.84(2.18)	3.94(3.94)	1.77(2.14)	2.38
4_0^+	0.50(0.63)	3.00(2.87)	0.46(0.59)	3.04(2.91)	1.73
5_0^+	0.13(0.19)	1.07(1.06)	0.13(0.18)	1.06(1.04)	—
6_0^+	0.07(0.07)	0.13(0.14)	0.07(0.07)	0.12(0.13)	1.01
3_3^+	1.39(2.11)	0.88(1.96)	1.32(2.07)	0.83(1.92)	1.68
3_3^-	12.14(11.35)	12.83(11.96)	11.70(10.93)	13.12(12.21)	14.23
4_3^-	2.47(2.56)	2.14(2.21)	2.52(2.59)	2.07(2.15)	4.90
4_3^+	0.66(0.76)	0.87(0.92)	0.65(0.75)	0.82(0.87)	2.70
5_3^+	0.11(0.13)	0.25(0.28)	0.10(0.12)	0.22(0.25)	—
5_3^-	0.66(0.71)	1.18(1.16)	0.63(0.69)	1.17(1.15)	—
6_3^-	0.06(0.09)	0.27(0.26)	0.06(0.09)	0.26(0.26)	—
6_3^+	0.01(0.02)	0.04(0.05)	0.01(0.02)	0.04(0.05)	—
6_6^-	0.04(0.07)	0.06(0.11)	0.04(0.06)	0.06(0.11)	—
6_6^+	0.38(0.39)	0.91(0.87)	0.41(0.43)	0.96(0.91)	—
7_6^+	0.12(0.12)	0.12(0.11)	0.11(0.12)	0.11(0.11)	—
7_6^-	0.01(0.01)	0.02(0.02)	0.01(0.01)	0.02(0.02)	—

[a] V_I, delta function model inversion, *ab initio* potential.
[b] V_{II}, delta function model inversion, scaled potential.
[c] V_{III}, "exact" inversion, *ab initio* potential.
[d] V_{IV}, "exact" inversion, scaled potential.

This would not be so in the first Born approximation. It means that the contributions from higher Born approximations are significant. The importance of higher order effects in the interaction between Ar and NH_3 is confirmed by calculations on bound states. Although the v_{33} term does not contribute to the lower bound states in a first order perturbation theory, which has the isotropic Hamiltonian as its zeroth order Hamiltonian, it proves to be one of the dominant terms in determining the rovibrational energy levels of the Ar–NH_3 complex.[12]

At the energies used here, application of the delta function model for the inversion of NH_3 has only a small effect on the cross sections, as compared to the "exact" calculations, in the order of 3%. The parity propensities, which

TABLE VI. State-to-state cross sections $\sigma(1_1^- \rightarrow j_k^e)$ for para-NH_3–Ar in Å^2. The relative kinetic energies are as indicated. The cross sections given in parentheses are corrected for the incomplete initial state preparation in the measurement, as follows [cf. Eq. (17)]: $\sigma(\rightarrow j_k^e) = 0.95\sigma(1_1^- \rightarrow j_k^e) + 0.05\sigma(1_1^+ \rightarrow j_k^e)$. A dash (—) in the last column indicates that the corresponding cross section has not been measured.

280 cm^{-1}				485 cm^{-1}			
j_k^e	V_{III}[a]	V_{IV}[b]	Expt.	j_k^e	V_{III}[a]	V_{IV}[b]	Expt.
2_1^-	4.22(4.23)	2.82(3.21)	4.70	2_1^-	3.62(3.66)	2.23(2.50)	5.51
2_+^1	4.40(4.39)	10.73(10.33)	6.32	2_1^+	4.39(4.35)	7.72(7.45)	3.76
3_1^+	2.00(2.06)	1.57(1.66)	0.89	3_1^+	1.65(1.73)	1.26(1.43)	1.35
3_1^-	3.35(3.28)	3.27(3.18)	1.35	3_1^-	3.24(3.17)	4.55(4.39)	1.37
4_1^-	0.57(0.56)	1.42(1.37)	—	4_1^-	1.10(1.06)	0.93(0.92)	—
4_1^+	0.33(0.34)	0.50(0.55)	—	4_1^+	0.27(0.32)	0.78(0.79)	—
2_2^-	0.99(1.61)	0.47(1.11)	1.19	2_2^-	0.62(1.12)	0.44(1.03)	1.50
2_2^+	13.48(12.85)	13.30(12.65)	12.94	2_2^+	10.52(10.03)	12.13(11.55)	7.70
3_2^+	2.64(2.70)	3.06(2.96)	3.24	3_2^+	1.96(2.06)	1.46(1.46)	4.26
3_2^-	3.90(3.84)	1.05(1.15)	2.56	3_2^-	3.94(3.84)	1.56(1.55)	1.95
4_2^-	0.52(0.52)	0.97(0.96)	0.97	4_2^-	0.79(0.79)	0.71(0.75)	1.19
4_2^+	0.59(0.58)	0.75(0.76)	—	4_2^+	0.71(0.71)	1.58(1.54)	—
5_+^2	0.12(0.12)	0.22(0.22)	—	5_2^+	0.36(0.35)	0.63(0.61)	—
5_2^-	0.03(0.04)	0.09(0.10)	—	5_2^-	0.14(0.15)	0.25(0.27)	—
4_4^-	0.69(0.72)	0.52(0.60)	0.80	4_4^-	0.56(0.62)	0.49(0.62)	1.24
4_4^+	1.25(1.23)	2.15(2.07)	2.43	4_4^+	1.72(1.66)	3.10(2.97)	2.11
5_4^+	0.39(0.39)	0.39(0.38)	0.44	5_4^+	0.44(0.45)	0.37(0.37)	1.25
5_4^-	0.42(0.42)	0.22(0.23)	—	5_4^-	0.49(0.48)	0.31(0.31)	0.75
5_5^+	0.22(0.24)	0.25(0.27)	—	5_5^+	0.40(0.43)	0.19(0.23)	—
5_5^-	0.54(0.52)	0.67(0.65)	—	5_5^-	0.94(0.92)	0.94(0.90)	—

[a] V_{III} "exact" inversion, *ab initio* potential.
[b] V_{IV}, "exact" inversion, scaled potential.

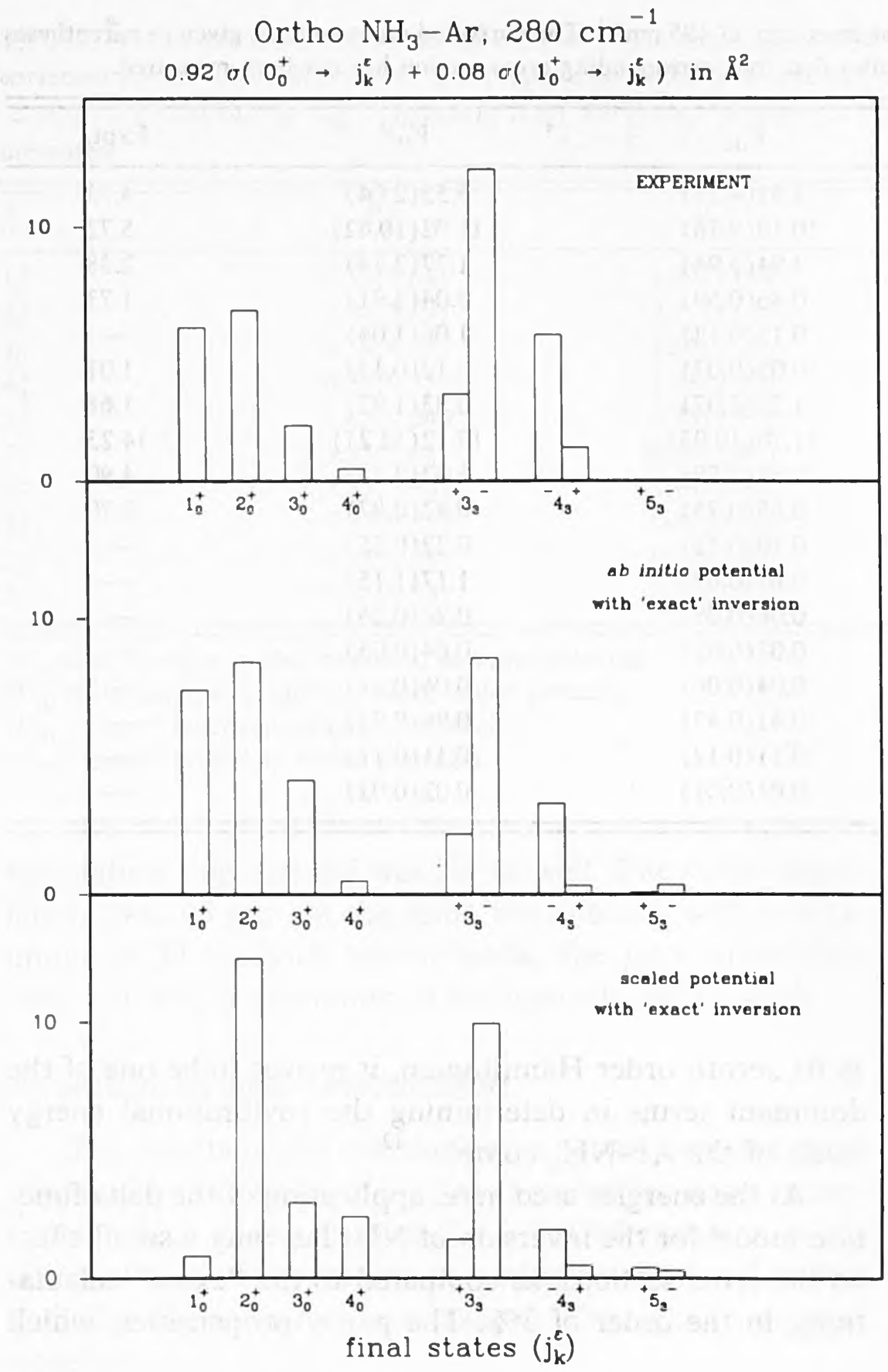

FIG. 2. Experimental and theoretical cross sections for ortho-NH_3 at a relative kinetic energy of 280 cm^{-1}. The theoretical values are given in parentheses in Table IV, for the 1_0^+ state we have used the expression given in that table.

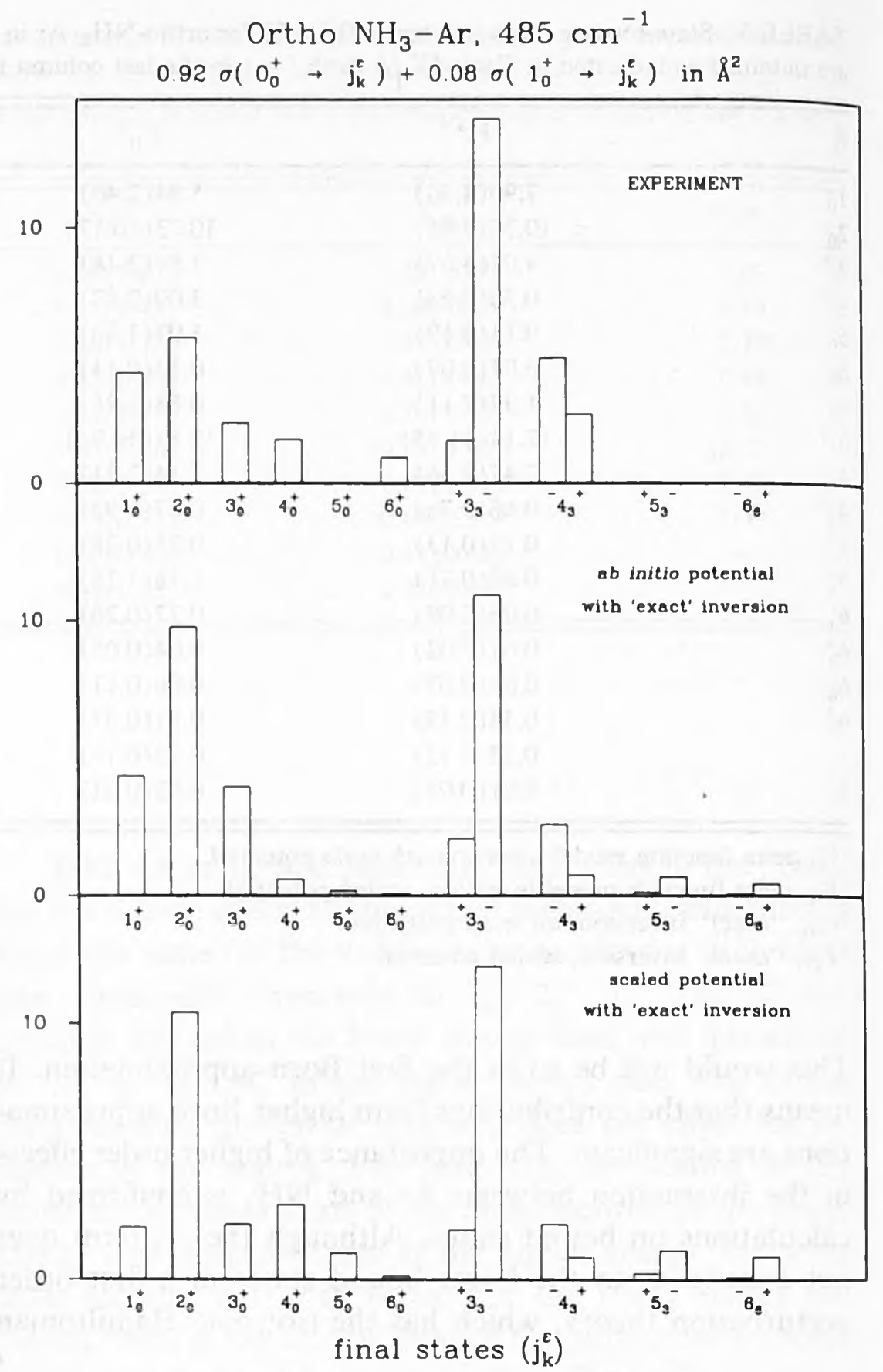

FIG. 3. Experimental and theoretical cross sections for ortho-NH_3 at a relative kinetic energy of 485 cm^{-1}. The theoretical values are given in parentheses in Table V, for the 1_0^+ state we have used the expression given in Table IV.

are defined as the ratios between the difference and the sum of the cross sections to the ± inversion states,[15] are hardly affected. The suggestion that deviations of theoretical propensities from experimental ones in He–NH_3 can be accounted for by taking the inversion motion explicitly into account[4,5] is hereby contradicted to all likelihood.

Our calculations show further that the invariance to a simultaneous change of parity in the incoming and outgoing channels [cf. Eq. (16)] for para-NH_3 holds to an accuracy of ~0.2% when the inversion is included in the potential matrix elements, but the inversion splitting of 0.8 cm^{-1} is neglected. When this splitting is included also, the deviations are of the order of 3%. Billing[18] has found in He–NH_3 calculations at an energy of 65 meV (525 cm^{-1}), using a semiclassical approach, that the invariance is obeyed to within 5% when the splitting of the inversion doublet is taken into account. The effect of including the tunneling splitting on the invariance is therefore larger than the effect of the "exact" calculation of potential matrix elements over the inversion wave functions.

The limited influence of the delta function model for inversion seems surprising at first sight, because the wave functions in Fig. 1 do not resemble delta functions. It means, however, as is noted by Davis and Boggs,[2] that the $v_{\lambda\mu}(R,\rho)$ are functions of ρ that vary slowly enough for the delta function approach to be valid.

Application of the CS approximation gives a reasonable agreement for para-NH_3 (Table VII). For ortho-NH_3, however, there are strong deviations, both from the CC method and from experiment. The CS calculation gives zero cross sections to the 3_3^+ and 4_3^+ states, whereas both experimental and CC cross sections to these states are different from zero. This means that these transitions are caused by the Coriolis terms in the Hamiltonian. Even though these terms are small, their long range apparently gives rise to significant transition probabilities.

In calculations on He–NH_3 scattering at an energy of 98 meV (792 cm^{-1}) using the CS method Meyer *et al.* have found the cross sections to the 3_3^+ and 4_3^+ states to be exactly zero and the cross section to the 2_2^- state to be

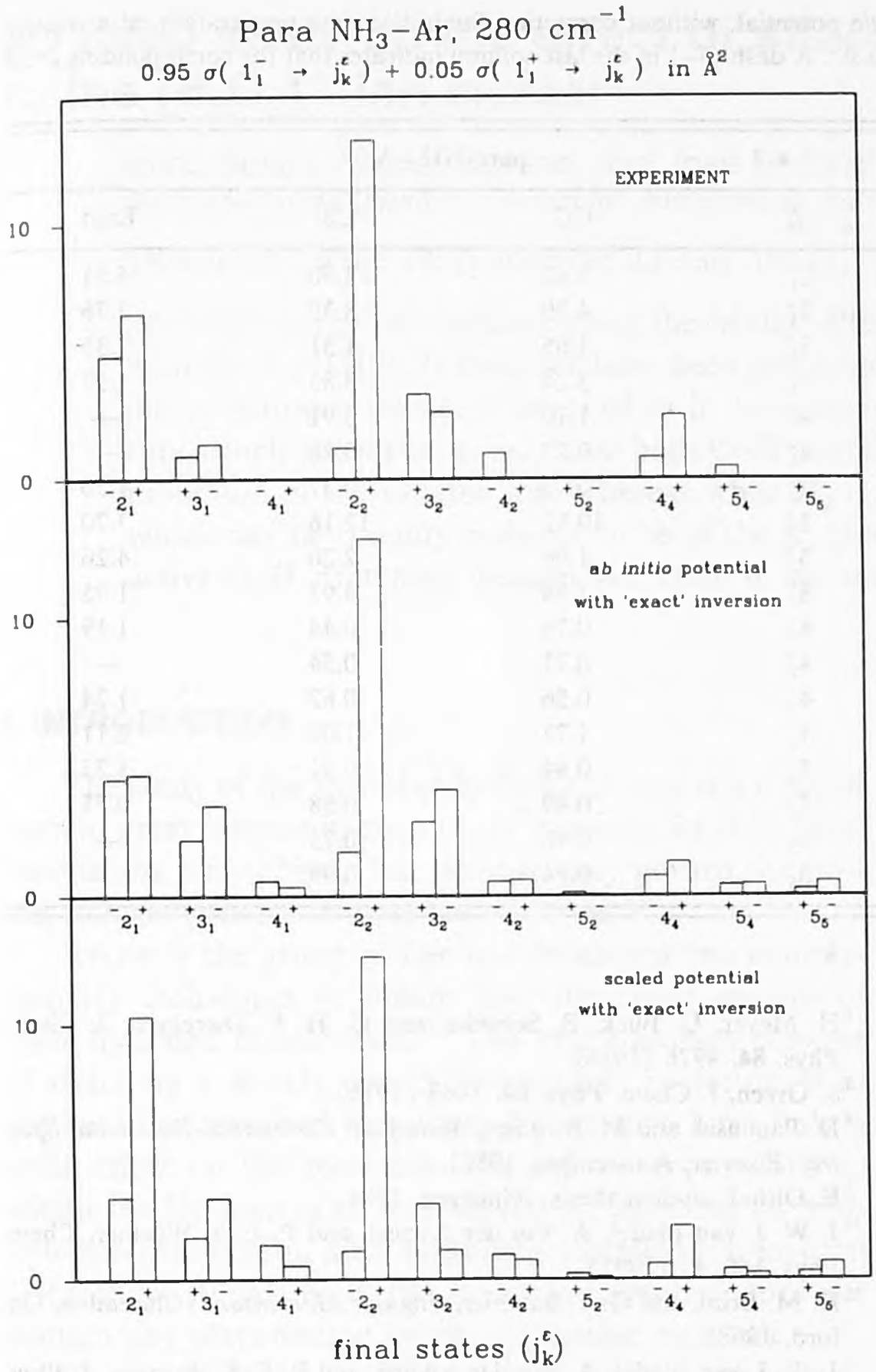

FIG. 4. Experimental and theoretical cross sections for para-NH_3 at a relative kinetic energy of 280 cm^{-1}. The theoretical values are given in parentheses in Table VI.

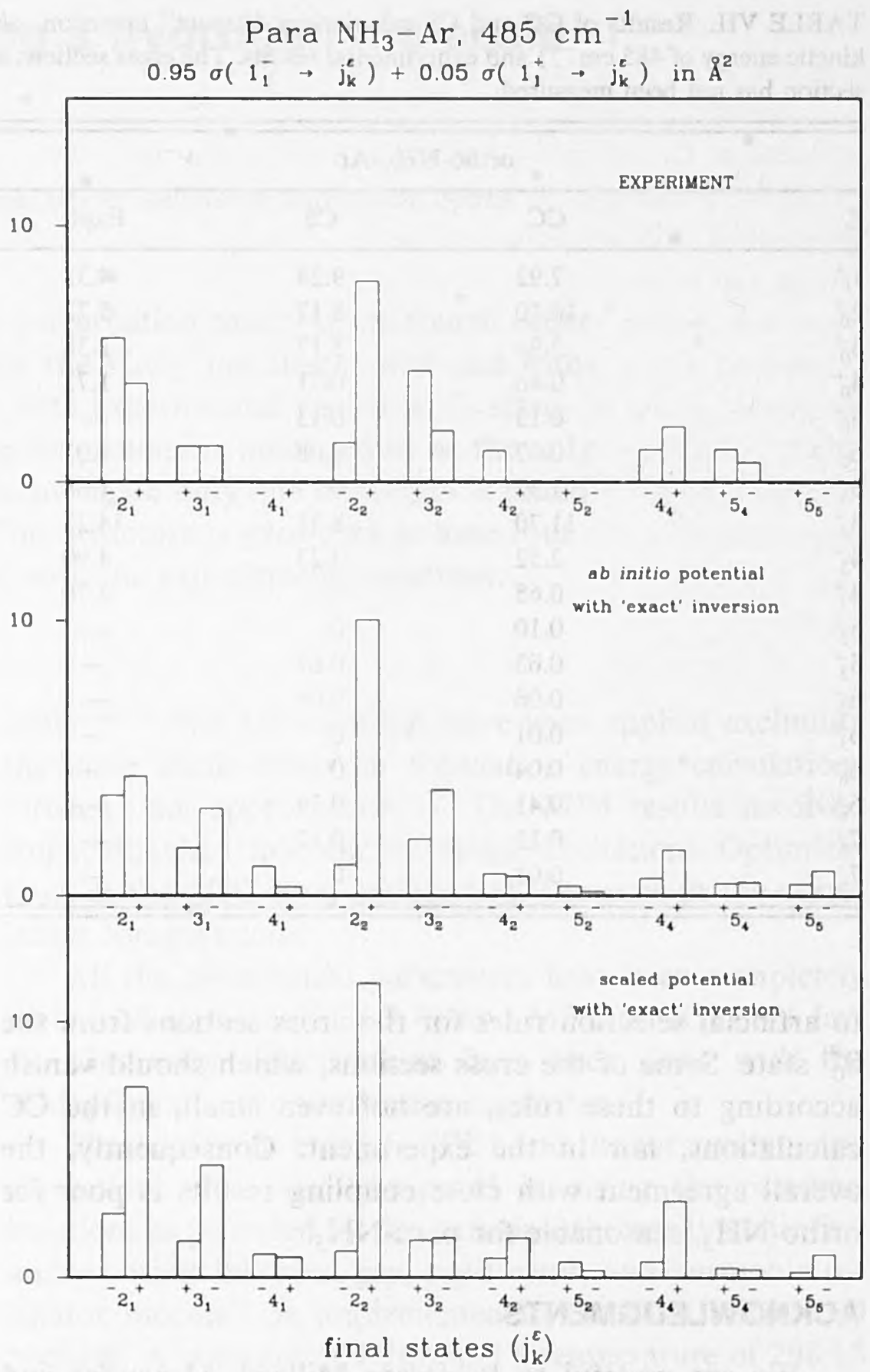

FIG. 5. Experimental and theoretical cross sections for para-NH_3 at a relative kinetic energy of 485 cm^{-1}. The theoretical values are given in parentheses in Table VI.

extremely small.[3] The fact that the 3_3^+ and 4_3^+ cross sections are zero is an artifact of the CS method. The smallness of the 2_2^- cross section, however, cannot be attributed to this method.

V. CONCLUSIONS

We have calculated close coupling state-to-state cross sections for the inelastic scattering of NH_3 with Ar at two different collision energies and compared them with experimentally derived cross sections. The inversion motion of NH_3 has been taken into account explicitly. Comparison with calculations that use a delta function model description of the inversion motion, shows that this model leads to errors of 3% only, at the energies used here. Previously found[4,5] deviations from experimentally determined parity propensities for NH_3–He, cannot be attributed to use of the delta function model. It is more likely that these discrepancies arise from shortcomings of the intermolecular potential used for that system.

In calculations on bound states of Ar–NH_3, the use of a potential in which a single term in the angular expansion of the *ab initio* potential of Ref. 1 was scaled by a factor of 1.43, gave better agreement with spectroscopic data than the use of the original *ab initio* potential. In the present scattering calculations the opposite is true. This can be seen as a manifestation of the fact that scattering and bound states probe different regions of the intermolecular potential surface. The applied scaling is too crude to obtain a fully realistic potential surface. For ortho-NH_3 the calculated *ab initio* cross sections reproduce the experimental ones fairly well. For para-NH_3 the overall agreement is good too, but differences remain between theoretical and experimental parity propensities, indicating that the *ab initio* potential needs further improvement.

Comparison of the results for the two potentials shows further that the cross sections are very sensitive to variations in the potential surface. The changes in the cross sections for transitions to the various rotation–inversion states induced by the scaling, show also that higher order effects play a role in the scattering process, just as they do in bound state interactions.

Application of the coupled states approximation leads

TABLE VII. Results of CC and CS calculations ("exact" inversion, *ab initio* potential, without correction for initial state preparation, at a relative kinetic energy of 485 cm^{-1}) and experimental results. The cross sections are in $Å^2$. A dash (—) in the last column indicates that the corresponding cross section has not been measured.

ortho-NH_3–Ar				para-NH_3–Ar			
j_k^ϵ	CC	CS	Expt.	j_k^ϵ	CC	CS	Expt.
1_0^+	7.92	9.24	4.33	2_1^-	3.62	3.30	5.51
2_0^+	10.10	8.17	5.72	2_1^+	4.39	3.39	3.76
3_0^+	3.94	5.17	2.38	3_1^+	1.65	1.31	1.35
4_0^+	0.46	0.71	1.73	3_1^-	3.24	3.35	1.37
5_0^+	0.13	0.13	—	4_1^-	1.10	0.91	—
6_0^+	0.07	0.08	1.01	4_1^+	0.27	0.28	—
3_3^+	1.32	0	1.68	2_2^-	0.62	0.37	1.50
3_3^-	11.70	8.71	14.23	2_2^+	10.52	12.16	7.70
4_3^-	2.52	3.23	4.90	3_2^+	1.96	2.26	4.26
4_3^+	0.65	0	2.70	3_2^-	3.94	4.93	1.95
5_3^+	0.10	0	—	4_2^-	0.79	0.44	1.19
5_3^-	0.63	0.61	—	4_2^+	0.71	0.54	—
6_3^-	0.06	0.06	—	4_4^-	0.56	0.62	1.24
6_3^+	0.01	0	—	4_4^+	1.72	1.08	2.11
6_6^-	0.04	0	—	5_4^+	0.44	0.41	1.25
6_6^+	0.41	0.39	—	5_4^-	0.49	0.58	0.75
7_6^+	0.11	0.12	—	5_5^+	0.40	0.23	—
7_6^-	0.01	0	—	5_5^-	0.94	0.99	—

to artificial selection rules for the cross sections from the 0_0^+ state. Some of the cross sections, which should vanish according to these rules, are not even small, in the CC calculations, nor in the experiment. Consequently, the overall agreement with close coupling results is poor for ortho-NH_3, reasonable for para-NH_3.

ACKNOWLEDGMENTS

We are grateful to Professor Millard Alexander and Dr. Pierre Valiron for making available the HIBRIDON computer program and to Dr. Pierre Valiron also for valuable discussions. This work is part of the research program of the "Stichting voor Fundamenteel Onderzoek der Materie (FOM)," which is financially supported by the "Netherlands Organization for Scientific Research (NWO)."

[1] M. Bulski, P. E. S. Wormer, and A. van der Avoird, J. Chem. Phys. **94**, 491 (1991).
[2] S. L. Davis and J. E. Boggs, J. Chem. Phys. **69**, 2355 (1978).
[3] S. Green, J. Chem. Phys. **73**, 2740 (1980).
[4] J. Schleipen and J. J. ter Meulen, Chem. Phys. **156**, 479 (1991).
[5] C. Rist, Ph.D. thesis, Grenoble.
[6] H. Meyer, U. Buck, R. Schinke, and G. H. F. Diercksen, J. Chem. Phys. **84**, 4976 (1986).
[7] S. Green, J. Chem. Phys. **64**, 3463 (1976).
[8] D. Papoušek and M. R. Aliev, *Molecular Vibrational–Rotational Spectra* (Elsevier, Amsterdam, 1982).
[9] E. Olthof, student thesis, Nijmegen, 1991.
[10] J. W. I. van Bladel, A. van der Avoird, and P. E. S. Wormer, Chem. Phys. **165**, 47 (1992).
[11] D. M. Brink and G. T. Satchler, *Angular Momentum* (Clarendon, Oxford, 1968).
[12] J. W. I. van Bladel, A. van der Avoird, and P. E. S. Wormer, J. Phys. Chem. **95**, 5414 (1991).
[13] HIBRIDON is a package of programs for the time-independent quantum treatment of inelastic collisions and photodissociation written by M. H. Alexander, D. Manolopoulos, H.-J. Werner, and B. Follmeg, with contributions by P. F. Vohralik, G. Corey, B. Johnson, T. Orlikowski, and P. Valiron.
[14] G. Danby, D. R. Flower, E. Kochanski, L. Kurdi, P. Valiron, and G. H. F. Diercksen, J. Phys. B **19**, 2891 (1986).
[15] J. Schleipen, J. J. ter Meulen, G. C. M. van der Sanden, P. E. S. Wormer, and A. van der Avoird, Chem. Phys. **163**, 161 (1992).
[16] C. A. Schmuttenmaer, R. C. Cohen, J. G. Loeser, and R. J. Saykally, J. Chem. Phys. **95**, 9 (1991).
[17] E. Zwart, H. Linnartz, W. L. Meerts, G. T. Fraser, D. D. Nelson, and W. Klemperer, J. Chem. Phys. **95**, 793 (1991).
[18] G. D. Billing, L. L. Poulsen, and G. H. F. Diercksen, Chem. Phys. **98**, 397 (1985).